Available online at www.sciencedirect.com
SCIENCE DIRECT
Bioorganic & Medicinal Chemistry
Bioorganic & Medicinal Chemistry 14 (2006) 1221–1228

3′-*N*-Alkylamino-3′-deoxy-*ara*-uridines: A new class of potential inhibitors of ribonuclease A and angiogenin

Tushar K. Maiti, Soumya De, Swagata Dasgupta* and Tanmaya Pathak*

Department of Chemistry, Indian Institute of Technology, Kharagpur 721302, India

Received 23 August 2005; revised 19 September 2005; accepted 20 September 2005
Available online 10 October 2005

Abstract—In this study, we report the inhibition of ribonuclease A (RNase A) by certain aminonucleosides. This is the first such instance of the use of this group of compounds to investigate the inhibitory activity of this protein. The compounds synthesized have been tested for their ability to inhibit the ribonucleolytic activity of RNase A by an agarose gel-based assay. A tRNA precipitation assay and inhibition kinetic studies with cytidine 2′,3′-cyclic monophosphate as the substrate have also been conducted for two of the compounds. Results indicate substantial inhibitory activity with inhibition association constants in the micromolar range. The experimental studies have been substantiated by docking of the aminonucleoside ligands to RNase A using AutoDock. We find that the ligands preferentially bind to the active site of the protein molecule with a favorable free energy of binding. The study has been extended to a member of the ribonuclease superfamily, angiogenin, which is a potent inducer of blood vessel formation. We show that the aminonucleosides act as potent inhibitors of angiogenin induced angiogenesis.

1. Introduction

The design of small molecule inhibitors of ribonuclease A (RNase A) provides a meaningful way to probe the biological actions of related enzymes of the ribonuclease superfamily. Angiogenin, a member of the RNase superfamily, is unique among RNases in that it is a potent inducer of angiogenesis in vivo.[1–3] It has 33% sequence identity and 65% homology to that of RNase A.[4] Its enzymatic properties are also distinctive, most remarkably, the ribonucleolytic activity of angiogenin toward standard RNase substrates is extremely weak and almost 10^5–10^6 times lower than that of RNase A.[5–7] In spite of its weak enzymatic activity, evidence from studies with variants and inhibitors indicates that the ribonucleolytic activity of angiogenin is crucial for its angiogenic activity.[8–10] Targeting the enzymatic site of angiogenin by designing low molecular weight inhibitors would thus be an indirect way to curb its angiogenic activity.

We choose bovine pancreatic RNase A as a convenient model system in the design of potential low molecular weight synthetic inhibitors of angiogenin. The ribonucleolytic center of RNase A/angiogenin is constituted of multiple subsites[11–14] that bind to the phosphate, base, and sugar components of the RNA molecule. The most important binding sites are the P_1 binding site where cleavage of the phosphodiester bond occurs. The B_1 binding site serves as a base recognition site whose ribose sugar unit is attached to the phosphate group via the 3′-oxygen atom. The B_2 site is the recognition site for the base in which the ribose sugar is attached to the phosphate bond via the 5′-oxygen atom. Generally the B_1 site has specificity toward pyrimidines and the B_2 site toward purines.[15] A schematic diagram of dinucleotide binding with RNase A and angiogenin is given in Figure 1. To date, many nucleotide-based small molecule inhibitors of RNase A have been identified.[16–19] These nucleotide-based inhibitors have close resemblance to the substrate of RNase A and thus act as substrate mimics. Recently, Kao et al.[20] and Jenkins and Shapiro[21] identified some non-nucleoside-based inhibitors of RNase A/angiogenin that are functionalized with carboxylic acid or sulfonic acid groups.

Abbreviations: RNase A, ribonuclease A; HSA, human serum albumin; 2′-CMP, cytidine-2′-mono phosphate; 3′-CMP, cytidine-3′-mono phosphate; 2′,3′ cCMP, cytidine 2′,3′ cyclic monophosphate; tRNA, transfer ribonucleic acid; Mes, 4-morpholine ethanesulphonic acid; NMR, nuclear magnetic resonance; HRMS, high resolution mass spectrometry; PDB, protein data bank; GA, genetic algorithm.

Keywords: Ribonuclease A; Angiogenin and angiogenesis; Aminonucleosides; Precipitation assay; AutoDock; Inhibition kinetics.

* Corresponding authors. Tel.: +91 3222 283306; fax: +91 3222 255303; e-mail: swagata@chem.iitkgp.ernet.in

0968-0896/$ - see front matter © 2005 Elsevier Ltd. All rights reserved.
doi:10.1016/j.bmc.2005.09.049

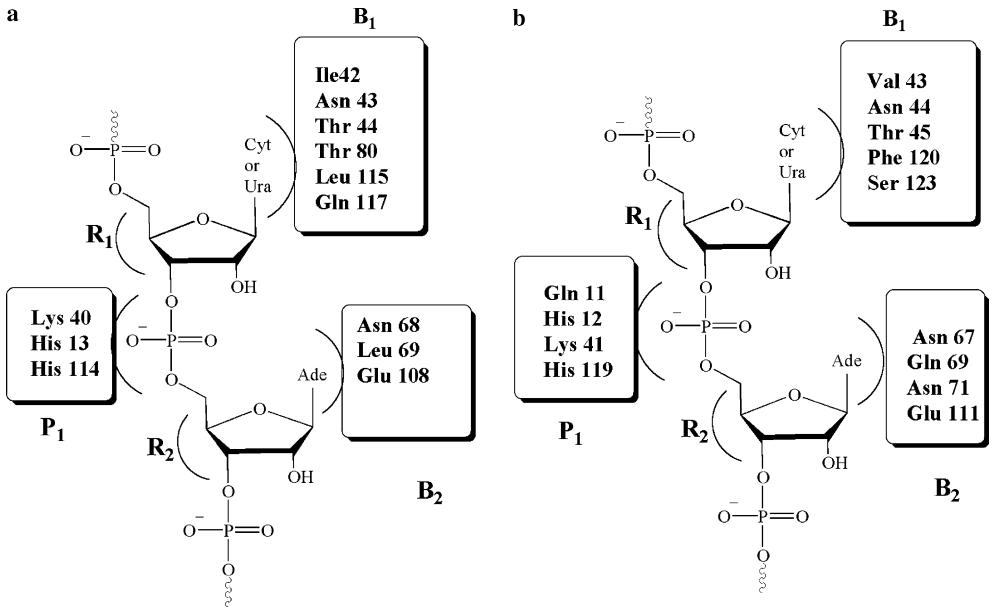

Figure 1. Schematic representation of the active center cleft in the (a) angiogenin–substrate complex and (b) RNase A–substrate complex. B, R, and P represent the base, ribose sugar, and phosphate binding subsites, respectively. B_1, R_1, and P_1 are the main binding sites at which the catalytic reaction takes place. In case of both proteins, B_1 prefers pyrimidines and B_2 prefers purines.

In the present study, we have synthesized specific aminonucleosides, which act as potent inhibitors of RNase A and angiogenin. Earlier reports indicate that the pK_a values of histidine residues present at the active site (His12 and His119) of RNase A change from ~5.22/6.78 for free enzymes to ~6.30/8.10 for enzyme–substrate complexes.[19] It is important to note that an overwhelming majority of small molecule-based RNase A/angiogenin inhibitors are functionalized with acidic groups such as phosphate, carboxylic or sulfonic acid moieties.[21] It is expected that at physiological pH these acidic groups would exist in the deprotonated form and would therefore interact electrostatically with the protonated basic groups present at the P_1 site.[22] In a departure from the standard approach of using acidic compounds, we opined that a uridine derivative functionalized with amino groups having basicities comparable (or higher) to those of the imidazole moiety of His12 and His119 should be able to perturb the protonating/deprotonating environment of the P_1 site. This phenomenon would, in turn, diminish the ribonucleolytic activity of RNase A. Moreover, it has been reported that the protonated forms of His12 and His119 contribute significantly to the stability of the RNase A-single stranded nucleic acid complex. Therefore, the presence of externally delivered stronger amino groups at the P_1 site may scavenge protons from His12 and His119, thereby adversely affecting the contributions of these amino acid residues toward the stability of the enzyme–natural substrate complex.

Here we report for the first time the use of aminonucleosides as effective inhibitors of the ribonucleolytic activity of RNase A. This has been extended to understanding the effect on the ribonucleolytic activity of angiogenin which, in turn, affects the biological activity of the protein. The potential antiangiogenic activity of the aminonucleosides has also been checked in a preliminary assay wherein blood vessel formation was inhibited. We believe that aminonucleosides could be used as effective model compounds to further design inhibitors in an attempt to check undesirable vascularization.

2. Results and discussion

A specific class of aminonucleosides carrying amino groups of pK_a values ranging from 8.70 to 10.92 was synthesized to study their efficacy as RNase A inhibitors. Compounds **3a**–**c** were synthesized as described in Scheme 1 following a reported procedure. Compounds **3d** and **3e** were synthesized from the known aminonucleoside **2d**. Inhibition of the ribonucleolytic activity of RNase A was initially checked by an agarose gel-based assay, where we monitored the degradation of tRNA by RNase A. Known inhibitors of RNase A, cytidine-2′-monophosphate (2′-CMP) and cytidine-3′-monophosphate (3′-CMP) were used to compare the inhibitory activities of the compounds in an agarose gel (Fig. 2). The most intense band observed is due to the presence of the control tRNA. The faint intensity of the band in lane 2 is due to the degradation of tRNA by RNase A alone. The differential intensity of bands in lanes 2, 3, and 5 qualitatively indicates the degree of RNase A inhibition of the compounds. In each case, lane 5 contains the synthesized compound. The relative intensity in lane 5 with the compounds is higher compared to that in lane 2 but less intense compared to those in lane 3 (2′-CMP) and lane 4 (3′-CMP). These results show, albeit qualitatively, that these compounds can act as effective inhibitors of RNase A. The efficacy of the inhibitors is in the order 2′-CMP > 3′-CMP > aminonucleosides for all the cases. Out of five aminonucleosides we

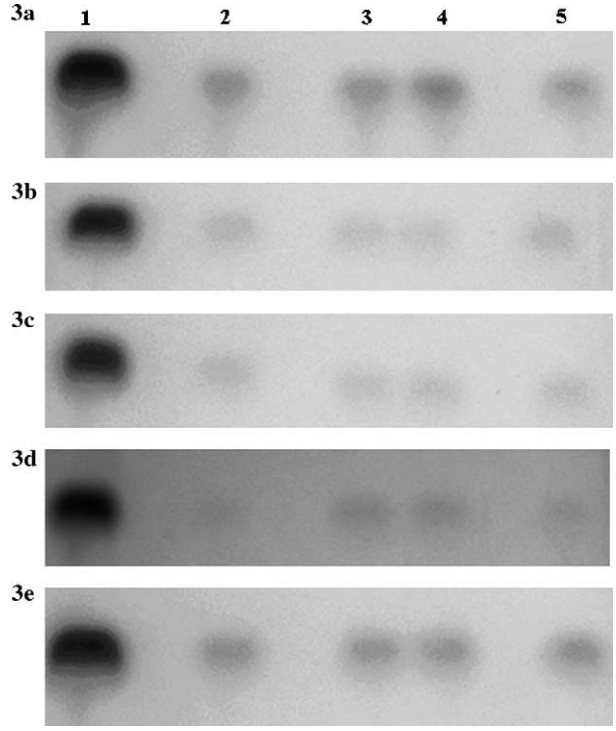

Figure 2. Agarose gel-based assay for the inhibition of RNase A by the synthesized compounds. Lane 1, tRNA; lane 2, RNase A + tRNA; lane 3, 2′-CMP, RNase A + tRNA; lane 4, 3′-CMP, RNase A + RNA; lane 5, synthesized compounds, RNase A + tRNA.

selected **3d** and **3e** for further analysis because: (a) **3d** in its ester form would behave more like a basic nucleoside and (b) the 3′ substitution in **3e** would exist in one of the three possible forms (basic/neutral/acidic) depending on the local pH of the P_1 site; other factors such as ring size, etc., would be comparable to those of **3d**. Moreover **3e**, in the deprotonated form, would be able to interact electrostatically with the protonated base residues present at the P_1 site.

The inhibition of ribonucleolytic activity of **3d** and **3e** was further checked by the precipitation assay. The plots of relative activity versus inhibitor concentration give us an idea of the relative inhibitory power of the inhibitors. Figure 3 shows the relative inhibitory efficacy of 2′-CMP, 3′-CMP, and **3d** and **3e**. The activity of RNase A is reduced by 30% with the following concentrations of each inhibitor, 3.55×10^{-5} M of 2′-CMP, 1.21×10^{-4} M of 3′-CMP, 4.03×10^{-4} M for **3d**, and 8.47×10^{-4} M for **3e**.

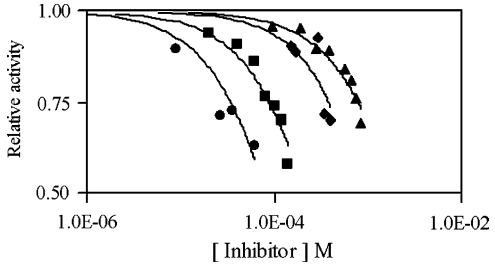

Figure 3. Relative activity plots of inhibition of RNase A by 2′-CMP (-●-), 3′-CMP (-■-), **3d** (-♦-), and **3e** (-▲-).

For determination of the inhibition constants of **3d** and **3e** by kinetic experiments, the reciprocal of reaction velocity has been plotted against inhibitor concentration for three different substrate concentrations (Fig. 4). The linear Dixon plot for the three different concentrations of the same substrate intersects at an inhibitor concentration equal to the negative reciprocal of the inhibitor association constant. For **3d**, the inhibition constant is found to be 120 μM. The inhibition constant for **3e** is 103 μM. Values for 2′-CMP and 3′-CMP are 7 and 103 μM, respectively. From these results we may conclude that **3d** and **3e** exhibit comparable activity toward RNase A as 3′-CMP.

To further substantiate this, we have performed docking studies with AutoDock. In the AutoDock docking procedure, the change in the receptor structure associated with ligand binding is not considered. We have docked both 2′-CMP and 3′-CMP along with **3d** and **3e** to wild type RNase A. The docked structures obtained from AutoDock agree well with the structures of RNase A complexed with 2′-CMP and 3′-CMP obtained from the Protein Data Bank (PDB entries 1JVU and 1RPF, respectively). From the docking studies we obtain the final docked energies as well as the estimated inhibition constants. The results are summarized in Table 1. Both the theoretical and experimental inhibition constants are found to be in the micromolar range. The difference between the experimental and theoretical values may be attributed to the fact that the AutoDock program treats the receptor molecule as rigid, whereas the ligand is flexible. The experimental inhibition constants for **3d** and **3e** are close to that of 3′-CMP. We expect the compounds to dock to the active site of the protein based on the competitive nature of inhibition obtained from the kinetic studies. As anticipated, **3d** and **3e** dock to the active site of the protein molecule that comprises His12, Lys41, Thr45, and His119. A surface representation of the protein molecule is shown with the compounds docked to the active site in Figure 5. The most conspicuous feature of the docked compounds is the reversed orientation of the two compounds with respect to each other. With the phosphate position modified, the recognition of the base appears to be less important for the accommodation of **3d** in the active site. For **3d**, Thr45, one of the key residues of the base recognition site, (Fig. 1b), is within hydrogen bonding distance of the C=O of the ester moiety of **3d**. The base is within interacting distance of Lys7 and Gln11. In contrast, **3e**, with a carboxylic acid moiety, is hydrogen bonded to Gln 11 through the carboxylic –OH. The P_1 recognition site comprising residues His12, Lys41, and His119 also recognizes **3e**. Of these, His12 and Lys41 are within hydrogen bonding distance of the carboxylic –OH. Even with the six-membered ring spanning the region between the sugar and the acid group Thr45 and Ser123 of site B_1 are able to serve as the recognition site for the base (Fig. 6). The flexible structure of **3e** with additional

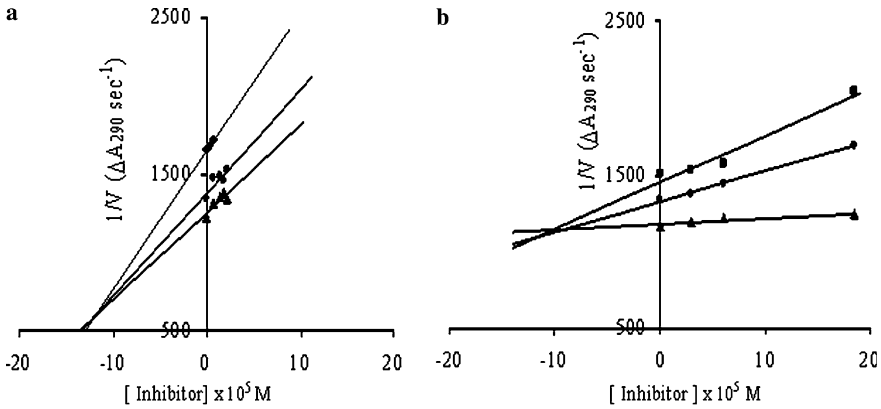

Figure 4. (a) Dixon plot for inhibition of RNase A (1.58 μM) by compound **3d**. Substrate concentrations are 0.4065 mM (■), 0.5421 mM (●), and 0.6775 mM (▲). (b) Dixon plot for inhibition of RNase A (0.64 μM) by compound **3e**. Substrate concentrations are 0.3423 mM (■), 0.4108 mM (●), and 0.6984 mM (▲).

Table 1. Comparison of binding constants and binding energies of the listed compounds

	2′-CMP	3′-CMP	**3d**	**3e**
Experimental K_i (M)	7.0×10^{-6} [a]	103×10^{-6} [a]	120.0×10^{-6} [b]	103.0×10^{-6} [b]
Theoretical K_i (M)	10.1×10^{-6}	30.6×10^{-6}	36.0×10^{-6}	0.09×10^{-6}

[a] Ref. 19.
[b] This study.

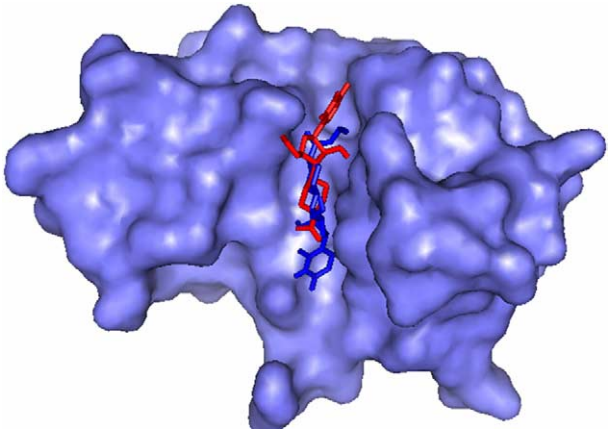

Figure 5. Surface representation of RNase A with **3d** (blue) and **3e** (red) docked. The cleft to which the compounds are bound is the substrate binding site of the protein. (For interpretation of the references to color in this figure legend, the reader is referred to the web version of this paper.)

puckering/bending of the backbone appears to permit this.

Encouraged by these findings, we checked whether the synthesized compounds were capable of inhibiting the ribonucleolytic activity of angiogenin. In a precipitation assay for monitoring the inhibition of the ribonucleolytic activity of angiogenin, we observed that compounds **3d** and **3e** inhibit 35% and 38% of the enzymatic activity, respectively. This implies that the angiogenic activity of angiogenin should also be affected owing to a disruption in the enzymatic activity due to the aminonucleosides. The chorioallantoic membrane assay was then conducted to verify the inhibition of angiogenin induced angiogenesis by **3d** and **3e**. Results of the CAM assay with the synthesized compounds, **3d** and **3e**, are shown in Figure 7. The assay shows that **3d** and **3e** are indeed capable of reducing blood vessel formation in the chorioallantoic membrane. We observe that compared to the control in Figure 7a, a greater vascularization is observed in Figure 7b as expected due to the presence of angiogenin. With only the compounds **3d** and **3e** the blood vessels tend to move away from the disk (Figs. 7c and e). However, in the presence of angiogenin along with the compound, there is close to normal blood vessel formation (Figs. 7d and f). The results indicate that the compounds **3d** and **3e** have the potential to be developed as antiangiogenic compounds.

The homology of RNase A and angiogenin permits us to assess the effect of synthesized compounds, which act as substrate mimics, on ribonucleolytic proteins with unusual biological activity. This study on the inhibition of members of the ribonuclease superfamily, RNase A, and angiogenin by aminonucleosides opens up a completely novel area for further investigation. Apart from inhibition of RNase A, which is comparable to that of 3′-CMP demonstrated by kinetic studies on the compounds, we observe a different binding mode for **3a**–**d**. Thus, it may be inferred that the recognition of the uracil moiety by Asn44/Asn43, Thr45/Thr44, Thr80/Asp83, and Phe120/Glu117 (B_1 site; Fig. 1) is not a prerequisite for a modified nucleoside to behave as an inhibitor of RNase A/angiogenin. It appears that these compounds could provide an insight into the design of potential lead compounds for antiangiogenic activity.

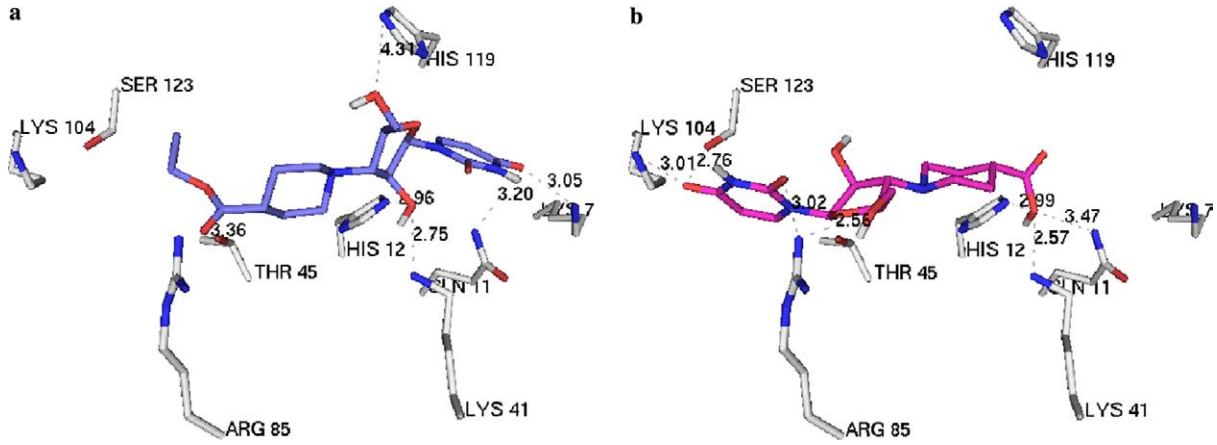

Figure 6. Lowest energy AutoDock poses of (a) **3d** and (b) **3e** in the RNase A active site. Side chains of the residues that contact the inhibitor are shown.

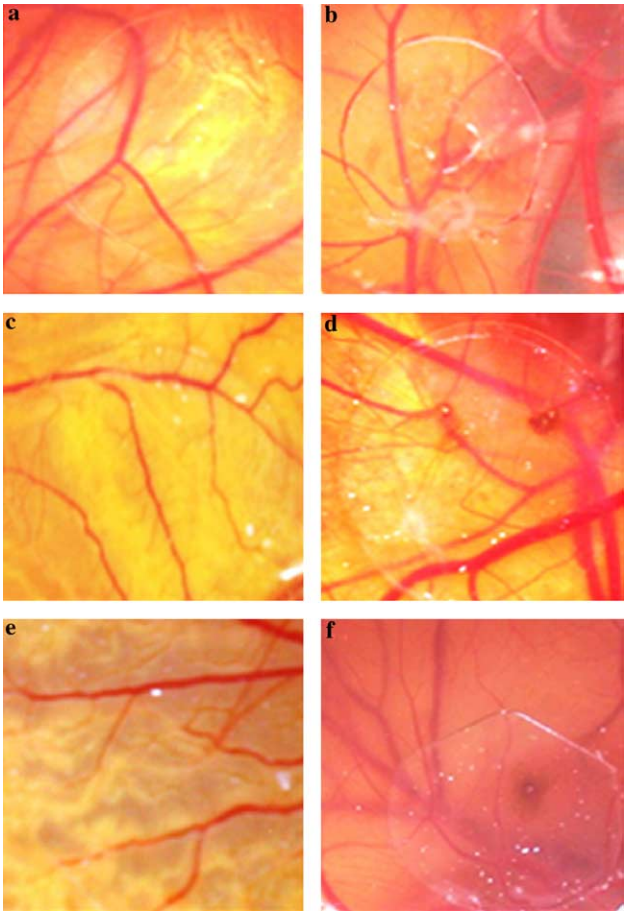

Figure 7. CAM assay with compounds **3d** and **3e** (a) control; with (b) angiogenin; (c) compound **3d**; (d) angiogenin + compound **3d**; (e) compound **3e**; (f) angiogenin + compound **3e**.

3. Materials and methods

3.1. Materials

Ribonuclease A (RNase A), yeast tRNA, human serum albumin (HSA), 2′,3′-cCMP, 2′-CMP, and 3′-CMP are from Sigma Aldrich. Column chromatographic separations were done using silica gel (Silica gel 60, 230–400 mesh, SRL India) or basic alumina (Brockmann Grade I for Chromatography, SRL India). All other chemicals are from SRL India. ^{1}H NMR (200 MHz) and ^{13}C NMR (50 MHz) spectra were recorded on a Bruker NMR spectrometer (δ scale). UV measurements were made using a Perkin-Elmer UV–Vis spectrophotometer (Model Lambda 25). Concentrations of RNase A, 2′,3′-cCMP, and 2′-CMP were determined spectrophotometrically using the following data: RNase A, $\varepsilon_{278.5} = 9800\ M^{-1}\ cm^{-1}$; 2′-3′-cCMP, $\varepsilon_{268} = 8500\ M^{-1}\ cm^{-1}$, and 2′-CMP, $\varepsilon_{260} = 7400\ M^{-1}\ cm^{-1}$.[23,24] Concentrations of the synthesized compounds were determined based on weight.

3.2. Synthesis of aminonucleosides

3.2.1. Compounds 3a–c. Compounds **3a**–**c** have been synthesized according to the procedure of Bera et al.[25] The *ara*-derivative **3d** and **3e** are synthesized as described here. The nucleophilic opening of the epoxide ring of **1** by ethyl nipecotate generated a mixture of *ara*- and *xylo*-derivatives in which the *ara*-derivative **2d** was the major component (Scheme 1).[25] Compounds **2d**, after separation by column chromatography, was converted to **3d** and **3e** as shown in Scheme 1.

3.2.2. Compound 3d. A solution of **2d** (0.5 mmol) in aqueous acetic acid (80%, 10 ml) was heated at 100 °C for 30 min. Acetic acid and water were removed under reduced pressure and the residual liquid was coevaporated twice with ethanol. The solid residue was triturated with ether to remove tritanol. The compound was dissolved in water and washed several times with ethyl acetate to remove the residual tritanol. The aqueous solution was lyophilized to get the title compound.

Yield: 75%, hygroscopic. ^{1}H NMR (D_2O): δ 7.85 (d, 8.1 Hz, 1H) H-6; 6.0 (d, 4.4 Hz, 1H), H-1′; 5.85 (d, 8.1 Hz, 1H) H-5; 4.61 (m, 1H); 4.16 (q, 3H); 3.97–3.76 (m, 2H); 3.13–2.90 (m, 3H); 2.44 (m, 3H); 2.0 (m, 2H); 1.72 (m, 2H); 1.24 (t, 3H). ^{13}C NMR (D_2O + DMSO-d_6): δ 175.5; 164.3; 149.4; 141.6; 98.9; 84.4; 77.5; 70.3; 69.2; 60.8; 59.9; 48.4; 47.4; 38.3; 25.3; 11.7. HRMS

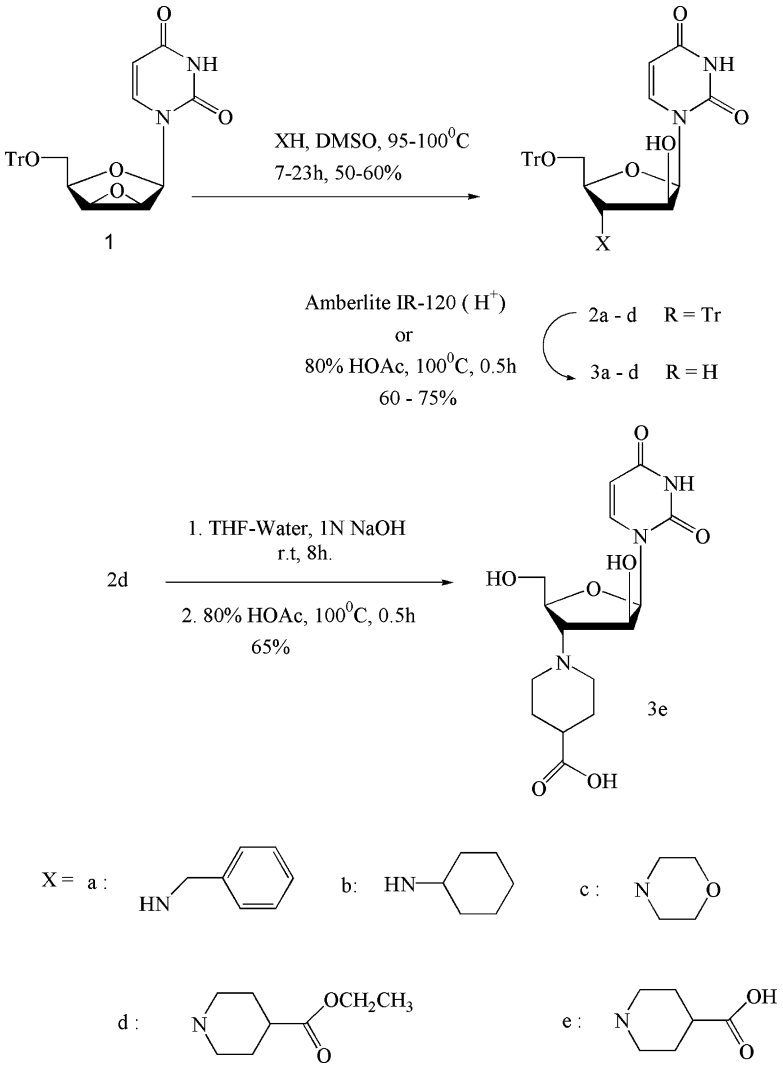

Scheme 1. Scheme for synthesis of the aminonucleosides.

(ES+ H)$^+$: calculated for $C_{17}H_{26}N_3O_7$: 384.1771. Found: 384.1763.

3.2.3. Compound 3e. To a solution of **2d** (0.5 mmol) in THF (10 ml), an aqueous solution of sodium hydroxide (1 N, 20 ml) was added and the solution was stirred for 8 h. The solution was neutralized by careful addition of 1 N HCl. The compound was extracted with dichloromethane and dried over anhydrous sodium sulfate. The dichloromethane was removed under reduced pressure. The residue was then treated with 80% acetic acid (10 ml) and heated at 100 °C for 30 min. Acetic acid and water were removed under reduced pressure and the residual liquid was coevaporated twice with ethanol. The solid residue was triturated with ether to remove tritanol. The compound was dissolved in water and washed several times with ethyl acetate to remove residual tritanol. The aqueous solution was lyophilized to get the title compound.

Yield: 65%, hygroscopic. ^{1}H NMR (D_2O): δ 7.81 (d, 8.0 Hz, 1H) H-6; 6.02 (d, 4.4 Hz, 1H), H-1′; 5.83 (d, 8.1 Hz, 1H) H-5; 4.75 (m, 1H); 4.24 (m, 1H); 3.99–3.78 (m, 2H); 3.33 (m, 3H); 2.78 (m, 2H); 2.34 (m, 1H); 2.06 (m, 2H); 1.79 (m, 2H). ^{13}C NMR (D_2O + DMSO-d_6): 164.4; 149.4; 141.5; 99.1; 84.2; 76.6; 69.7; 69.3; 60.3; 49.2; 48.7; 40.6; 25.7. HRMS (ES+ H)$^+$: calculated for $C_{15}H_{22}N_3O_7$: 356.1458. Found: 384.1447.

3.3. Agarose gel-based assay

Inhibition of RNase A was checked qualitatively by the degradation of tRNA in an agarose gel. In this method, 20 μl of RNase A (0.011 mM) was mixed with 20 μl **3a**–**e** (0.42 mM), 2′-CMP (0.3138 mM), and 3′-CMP (0.3138 mM), respectively, and the resulting solutions were incubated for 2 h. Twenty microliter aliquots of the incubated mixtures were mixed with 20 μl tRNA (5 mg/ml tRNA freshly dissolved in RNase free water) and incubated for another 30 min. Ten microliter of sample buffer, which consists of 10% glycerol and 0.025% bromophenol blue in water, was added to the mixture and 15 μl of it extracted and loaded onto a 1.1% agarose gel. The residual tRNA was visualized after ethidium bromide staining under UV light.

3.4. Inactivation of RNase A by aminonucleosides

Inhibition of ribonucleolytic activity of RNase A was assayed by the precipitation assay as described by Bond.[26] In this method, RNase A (0.012 mM) was mixed with varying concentrations of compound **3d** (0.2217–5.744 mM) and **3e** (0.4706–3.7648 mM), and incubated for 2 h. Twenty microliters of the resulting solution was then mixed with 40 μl tRNA (5 mg/ml tRNA freshly dissolved in RNase A free water), 40 μl of Tris–HCl buffer of pH 7.5 containing 5 mM EDTA and 0.5 mg/ml HSA. After incubation of the reaction mixture at 25 °C for 30 min, the reaction was quenched by adding 200 μl ice-cold 1.14 N perchloric acid containing 6 mM uranyl acetate. The solution was kept in ice for another 30 min and centrifuged at 4 °C at 12,000 rpm for 5 min. One hundred microliters of the supernatant was taken and diluted to 1 ml. The change in absorbance at 260 nm was measured and compared to that of a control set.

3.5. Inhibition kinetics

The inhibition of RNase A by **3d** and **3e** was assessed by a spectrophotometric method as described by Anderson et al.[17] The assay was performed in 0.1 M Mes–NaOH buffer of pH 6.0 containing 0.1 M NaCl using 2′,3′-cCMP as the substrate. The substrate concentration ranged from 0.4065 to 0.6775 mM and the concentration of **3d** varied from 0 to 0.228 mM. The enzyme concentration for **3d** was 1.583 μM. For **3e**, the concentrations ranged from 0 to 0.185 mM with substrate concentrations ranging from 0.3423 to 0.6984 mM. In this case, the enzyme concentration was 0.634 μM. The inhibition association constants were determined from initial velocity data. The reciprocal of initial velocity is plotted against inhibitor concentration at a constant substrate concentration according to the equation:

$$\frac{1}{V} = \frac{(K_M + [S])}{V_S[S]} + \frac{K_M[I]}{K_i V_S[S]},$$

where V is the initial velocity, V_S is the final velocity, [S] is the substrate concentration, and [I] the inhibitor concentration, K_M is the Michaelis constant, and K_i is the inhibition association constant. The linear plots of each substrate concentration intersect at an inhibitor concentration equal to the negative reciprocal of the inhibition association constant, K_i.

3.6. Molecular docking

The crystal structure of wild type RNase A (PDB entry 1FS3) was downloaded from the Protein Data Bank[27] and used for docking studies. The coordinate files of the three dimensional structures of **3d** and **3e** were generated by CORINA (http://www2.ccc.unierlangen.de/software/corina/corina.html). Waters were removed from protein PDB files, polar hydrogen atoms added, and Kollman United Atomic (KOLLUA) charges assigned. Rotatable bonds in the ligands were assigned with Auto Dock Tools—an accessory program that allows the user to interact with AutoDock[28–30] from a Graphic User Interface. Ligand docking was carried out with the AutoDock 3.0.5 Lamarckian Genetic Algorithm (GA). The approximate binding free energies calculated by this program are based on an empirical function derived by linear regression analysis of protein–ligand complexes with known binding constants. This function includes terms for changes in energy due to van der Waals, hydrogen bonding, and electrostatic forces, as well as ligand torsion and desolvation. The docked energy also includes the ligand internal energy or the intramolecular interaction energy of the ligand.

Two sets of docking were performed. In the first set, the whole protein was enclosed in the grid defined by AutoGrid. The grid size was $90 \times 90 \times 90$ Å^3 with a grid spacing of 0.375 Å, centered on the protein. Step sizes of 1 Å for translation and 50° for rotation were chosen. The maximum number of energy evaluations was set to 2×10^6. Twenty runs were performed. For each of the 20 independent runs, a maximum number of 27,000GA operations were generated for a single population of 50 individuals. Once the binding site of the compounds was ascertained, the active site of the protein was enclosed with the grid. A grid size of $80 \times 80 \times 80$ Å^3 with a grid spacing of 0.297 Å, centered at the ligand, was used. Thirty runs were performed. The final docked energy has been considered in each case as the criterion for the best-docked conformation of the compound to the macromolecule. The AutoDock suite of programs considers a flexible ligand with a rigid receptor. Hence, we do not expect the experimental inhibition constant values of the synthesized compounds to absolutely agree with the theoretical values. However, to observe the trends in the experimental and theoretical values, we have used AutoDock to dock the known inhibitors 2′-CMP and 3′-CMP with RNase A apart from **3d** and **3e**. The final docking energy values and estimated inhibition constants obtained were recorded and compared with the experimental values in all the cases. The output from AutoDock was rendered with PyMol.[31] PyMol was also used to calculate the distances between possible hydrogen bonding partners.

3.7. Inhibition of ribonucleolytic activity of angiogenin

The effect of **3d** and **3e** on the ribonucleolytic activity of the angiogenin was examined with yeast tRNA as the substrate as described by Bond.[26] The protein angiogenin (0.5 ng) and its mixture with **3d** (3.4 ng) and **3e** (3.4 ng) were added separately to the assay mixture containing 1 μg of yeast tRNA, in 0.1 M Tris, pH 7.5, 5 mM EDTA, and 0.1 μg HSA in a final volume of 50 μl. After incubation for 4 h at 37 °C, 100 μl of 1.14 N perchloric acid containing 6 mM uranyl acetate was added, kept in ice for 30 min, and then centrifuged at 10,000 rpm for 5 min at 4 °C. One hundred microliters of supernatant was taken and diluted to 500 μl. The change in absorbance at 260 nm was measured and compared to a control set.

3.8. Angiogenic activity

Angiogenesis was assessed by using the chick embryo chorioallantoic membrane (CAM) assay method of Knighton et al.[32] as described in Fett et al.[3] In brief, the method is as follows. Fertilized chicken eggs were kept in the incubator at 37 °C for 2 days after which 1 ml of albumin was aspirated from the eggs. The CAM of the chicken eggs was exposed by carefully cutting a small hole through the shell on day 5. Ten microliter aliquots of angiogenin, **3d** and **3e**, and protein mixed with **3d** and **3e** were placed on transparent plastic disks and dried under laminar flow. The disks were inverted over the CAM on day 10 and the response was assayed microscopically after 48 h. The density of blood vessel formation in each case is assessed by comparing with that of a control set.

Acknowledgments

S.D.G. and T.P. are grateful to Department of Science and Technology (DST), Government of India, for financial support (SR/S5/OC-13/2002). T.K.M. thanks CSIR for a Senior Research Fellowship.

References and notes

1. Folkman, J.; Klagsbrun, M. *Science* **1987**, *235*, 442.
2. Riordan, J. F. In *Ribonucleases: Structure and Function*; D'Alessio, G., Riordan, J. F., Eds.; Academic press: New York, 1997, pp 445–489.
3. Fett, J. W.; Strydom, D. J.; Lobb, R. R.; Alderman, E. M.; Bethune, J. L.; Riordan, J. F.; Vallee, B. L. *Biochemistry* **1985**, *24*, 5480.
4. Kurachi, K.; Davie, E. W.; Strydom, D. J.; Riordan, J. F.; Vallee, B. L. *Biochemistry* **1985**, *24*, 5494.
5. Shapiro, R.; Riordan, J. F.; Vallee, B. L. *Biochemistry* **1986**, *25*, 3527.
6. Shapiro, R.; Weremowicz, S.; Riordan, J. F.; Vallee, B. L. *Proc. Natl. Acad. Sci. U.S.A.* **1987**, *84*, 8783.
7. Harper, J. W.; Vallee, B. L. *Biochemistry* **1989**, *28*, 1875.
8. Shapiro, R.; Fox, E. A.; Riordan, J. F. *Biochemistry* **1989**, *28*, 1726.
9. Shapiro, R.; Vallee, B. L. *Biochemistry* **1989**, *28*, 7401.
10. Curran, T. P.; Shapiro, R.; Riordan, J. F. *Biochemistry* **1993**, *32*, 2307.
11. Raines, R. T. In *Artificial Nucleases*; Zenkova, M. A., Ed.; Springer: Heidelberg, 2004, pp 19–32.
12. Russo, N.; Acharya, K. R.; Vallee, B. L. *Proc. Natl. Acad. Sci. U.S.A.* **1996**, *93*, 804.
13. Nogue's, M. V.; Vilanova, M.; Cuchillo, C. M. *Biochim. Biophys. Acta* **1995**, *1253*, 16.
14. Iwahashi, K.; Nakamura, K.; Mitsui, Y.; Ohgi, K.; Irie, M. *J. Biochem.* **1981**, *90*, 1685.
15. Fisher, B. M.; Grilley, J. E.; Raines, R. T. *J. Biol. Chem.* **1998**, *273*, 34134.
16. Russo, A.; Acharya, R. K.; Shapiro, R. *Method Enzymol.* **2001**, *341*, 629.
17. Anderson, D. G.; Hammes, G. G.; Walz, F. G. *Biochemistry* **1968**, *7*, 1637.
18. Raines, R. T. *Chem. Rev.* **1998**, *98*, 1045.
19. Herries, D. G.; Mathias, A. P.; Rabin, B. R. *Biochem. J.* **1962**, *85*, 127.
20. Kao, R. Y.; Jenkins, J. L.; Olson, K. A.; Key, M. E.; Fett, J. W.; Shapiro, R. *Proc. Natl. Acad. Sci. U.S.A.* **2002**, *99*, 10066.
21. Jenkins, J. L.; Shapiro, R. *Biochemistry* **2003**, *42*, 6674.
22. Silverman, R. B. In *The Organic Chemistry of Drug Design and Drug Action*; Elsevier: New York, 2004, p 126.
23. Sela, M.; Anfinsen, C. B. *Biochim. Biophys. Acta* **1957**, *24*, 229.
24. Brown, D. M.; Magrath, D. I.; Todd, A. R. *J. Chem. Soc.* **1952**, 2708–2714.
25. Bera, S.; Pathak, T.; Langley, G. J. *Tetrahedron* **1995**, *51*, 1459.
26. Bond, M. D. *Anal. Biochem.* **1988**, *173*, 166.
27. Berman, H. M.; Westbrook, J.; Feng, Z.; Gilliland, G.; Bhat, T. N.; Weissig, H.; Shindyalov, I. N.; Bourne, P. E. *Nucleic Acids Res.* **2000**, *28*, 235.
28. Morris, G. M.; Goodsell, D. S.; Halliday, R. S.; Huey, R.; Hart, W. E.; Belew, R. K.; Olson, A. J. *J. Comp. Chem.* **1998**, *19*, 1639.
29. Morris, G. M.; Goodsell, D. S.; Huey, R.; Olson, A. J. *J. Comput. Aided Mol. Des.* **1996**, *10*, 293.
30. Goodsell, D. S.; Olson, A. J. *Proteins: Struct., Funct., Genet.* **1990**, *8*, 195.
31. DeLano, W. L. In *The PyMOL Molecular Graphics System*; DeLano Scientific: San Carlos, CA, USA, 2005. <http://www.pymol.org/>.
32. Knighton, D.; Ausprunk, D.; Tapper, D.; Folkman, J. *Br. J. Cancer* **1977**, *35*, 347.